

Calculation of On-offshore Sand Movement and Wave Deformation on Two-dimensional Wave-current Coexistent System

Koichi Kinose* ,Shuji Okushima* and Masahito Tsuru**

Abstract

In this paper, we proposed a method of calculation to predict quantitatively the on-offshore sand movement and the wave deformation on a wave-current coexistent system by assuming a river mouth. And the calculated results were compared with the experimental data obtained for the coexistent system in a two-dimensional wave tank. The distribution of wave height on the breaker zone was analyzed by use of BORE MODEL. It was required for the calculation of the sand transport rate. The model was established on the assumption that the value of energy loss in a breaking wave was equivalent to that of bore. The wave height distribution on the offshore side of breaking point was presumed employing the third order approximate solution of Stokian wave on the coexistent system. The breaking point was obtained by use of Miche's criteria equation. The local sand transport rate could be calculated by use of POWER MODEL. The predominant direction of sand drift was recognized using relations for judgement which were derived from the experimental results. The transformation of sea bottom and river one was estimated on the basis of the calculated distributions of the wave height and the sand transport rate. The results obtained by this analytical method agreed well with the experimental results.

I. Introduction

In order to perform studies about closure of river mouth by sand drift, it is necessary to have a deep understanding of wave deformation and sand movements on a wave-current coexistent system where waves and the steady flow interact. Inman and Bowen¹⁾, Abou-Seida²⁾ and Tanaka et al.³⁾ have made experiments on

* National Research Institute of Agricultural Engineering
2-1-2, Kannondai, Tsukuba-shi, Ibaraki, 305 Japan.

** Department of Civil Engineering, Science University of Tokyo

sand transport rates and shapes of ripples under wave-current coexistent system. Watanabe⁴⁾ proposed a bed load formula applicable to coexistent system on the basis of a power model. Jonsson⁵⁾ and Sakai et al.⁶⁾ have calculated wave shoaling on coexistent system. In the present work, we will try as the initial step to construct a model simulating the on-offshore sand movement, the wave deformation due to wave and steady flow, and the two-dimensional bottom transformation. For this analysis, we considered the wave-current coexisting system by assuming a river mouth as shown in Fig.1. In addition, the results will be compared with the experimental data measured in a wave tank.

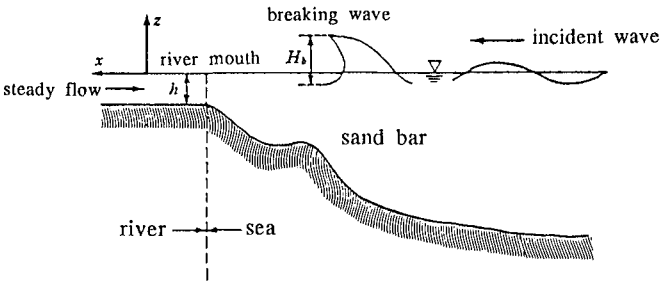


Fig.1 Wave-current coexistent system assumed to be river mouth.

II. Distribution of on-offshore sand transport rate

The sand transport rate on the wave-current coexistent system will be discussed in this chapter for the estimation of sea and river mouth bottom transformation.

2.1 Bed load formula

The local transport rate of bed load at a given point could be estimated by use of the power model proposed by Watanabe⁴⁾. The transport rate per unit width, q_{net} , can be obtained as the sum of the component q_w caused by wave motion and the component q_f caused by steady flow.

$$\begin{aligned}
 q_f &= A_f \frac{\tau - \tau_c}{\rho g} U_f \\
 q_w &= A_w \frac{\tau - \tau_c}{\rho g} U_w
 \end{aligned}
 \tag{1}$$

where A_w and A_f are non-dimensional constants, respectively, which are to be determined from laboratory or field data, τ is the maximum bed shear stress, τ_c is the critical shear stress, ρ is the fluid density, and g is the acceleration of gravity. U_f is the velocity of the steady flow and U_w is the bottom velocity amplitude of

orbital motion induced by wave. The critical shear stress can be obtained from the critical Shields parameter ψ_c ⁴⁾.

$$\begin{aligned}\psi_c &= 0.11 \text{ for } d/\delta_L < 1/6.5 \quad (\text{fine sand}) \\ \psi_c &= 0.06 \text{ for } d/\delta_L > 1/4.0 \quad (\text{coarse sand}) \quad (2) \\ \psi_c &= \frac{\tau_c}{\rho s g d}, \quad \delta_L = \sqrt{\frac{\nu T}{\pi}}\end{aligned}$$

where d is the median diameter of the sand, s is the specific gravity of immersed sand, δ_L is the thickness parameter of the boundary layer, ν is the kinematic viscosity of the fluid, and T is the wave period. When the diameter is intermediate between fine sand and coarse sand, the value of ψ_c is determined by interpolation. The value of q_w and q_f given by equation(1) are the net transport rate. On the assumption of a rough bottom, the value of τ can be obtained from the friction law proposed by Tanaka and Shuto⁵⁾ for the coexistent system. The friction law is shown in the Appendix.

Based on the above discussion, the local net transport rate, q_{net} , is given by

$$q_{net} = q_f + q_w \quad (3)$$

2.2 Expression of velocity field

By analogy with the analysis of phenomena in the vicinity of river mouth, the direction of the steady flow is considered to be offshore. Assuming that waves progress up a steady flow, the bottom velocity amplitude of orbital motion induced by the wave can be indicated from a small amplitude wave theory.

$$U_w = \frac{\pi H/L(L/T + U_f)}{\sinh kh} \quad (4)$$

where H is the wave height, h is the water depth, and L , k are the wave length and the wave number, respectively. The values of L and k are given by the following equations.

$$\begin{aligned}C &= \frac{L}{T} + U_f = \left(\frac{g L}{2\pi} \tanh kh \right)^{1/2} \\ k &= \frac{2\pi}{L}\end{aligned} \quad (5)$$

where C is the relative wave celerity to the steady flow. If the velocity of the steady flow exceeds a critical value, the wave does not progress up the steady flow. Its critical velocity U_{fc} can be obtained by

$$U_{fc} = \frac{C_0}{4} \tanh kh \quad (6)$$

where C_0 is the wave celerity at the deep water free from the effect of the steady flow. When $U_f > U_{fc}$, it is assumed that only the steady flow acts as the driving force of sand drift.

On the other hand, the vertically averaged velocity, U_f , is used for the calculation of the sand drift component, q_f . That is,

$$U_f = \frac{q_c}{h} \quad (7)$$

where q_c is the discharge per unit width.

2.3 Judgment of predominant direction of sand drift

The direction of the sand drift, q_f , is offshore, because the flow direction is considered to be offshore like that in the river mouth. But the predominant direction of q_w does not necessarily coincide with the direction of wave progress. Sunamura⁶⁾ has indicated that the direction of sand drift might change under the condition where equation(8) is satisfied.

$$\Phi = \gamma U_{r0} \quad (8)$$

where γ is an empirical constant, Φ is Hallermeier's parameter, and U_{r0} is Ursell parameter. They are expressed as follows by the long wave assumption, respectively.

$$\Phi = \frac{H^2}{s d h} \quad , \quad U_{r0} = \frac{g T^2 H}{h^2} \quad (9)$$

However, equation(8) is found from an experimental study of an uniformly sloping movable bed in a non-coexistent system where only wave acts. Sunamura has concluded that γ was equal to 0.13 on the surf zone in his experiments.

Taking the effect of the steady flow into consideration, equations(8) and (9) must be modified for the analysis of the wave-current coexistent system. The Ursell parameter on the coexistent system is shown as the following equation by applying the long wave assumption to the wave celerity, C , in the equation(5).

$$U_r = U_{r0} \left(1 - \frac{1}{2} \frac{H}{h} \frac{U_f}{U_w} \right)^2 \quad (10)$$

The relative intensity U_f/U_w in the above equation, which indicates a relative intensity ratio of the steady flow to the wave, was introduced for the judgment of the predominant direction of the sand drift, q_w . Using these parameters the judgment can be done as the follows. The zone of sand movement by wave and steady flow is divided into two regions; *pre-breaking* and *post-breaking region*.

In the post-breaking region, the values of Φ and U_r are calculated by use of equations(9) and (10), respectively, and a point, x_h , where the relation of Φ and U_r satisfies equation(11), is searched.

$$\Phi = \gamma U_r \quad (11)$$

Here, the value of U_f/U_w at point x_h is supposed to be β .

The direction of sand drift, q_w , induced by wave motion can be recognized using relations in equation(12).

$$\begin{aligned} \text{if } \beta > 0.15 & \quad \text{then offshore for all over the surf zone} \\ \text{if } \beta \leq 0.15 \text{ and } U_f/U_w > \beta & \quad \text{then offshore at a given point.} \\ \text{if } \beta \leq 0.15 \text{ and } U_f/U_w \leq \beta & \quad \text{then onshore at a given point.} \end{aligned} \quad (12)$$

In the pre-breaking region, we employ the relations shown in equation(13) .

$$\begin{aligned} \text{if } U_f/U_w > 0.15 & \quad \text{then offshore at a given point.} \\ \text{if } U_f/U_w \leq 0.15 & \quad \text{then onshore at a given point.} \end{aligned} \quad (13)$$

The critical value (0.15) of β could be given from the results of our previous experimental study⁷⁾.

III. Wave deformation of incoming waves on coexistent system

The wave height variation due to changes of depth and velocity of the steady flow will be considered. The zone of wave deformation is also divided into two regions; *pre-breaking* and *post-breaking region*.

3.1 Wave shoaling and breaking criterion

In the pre-breaking region, we employ the equation given by Sakai, Saeki and Ozaki⁸⁾ to calculate the wave deformation. This equation is the third order approximate solution of Stokian wave on the wave-current coexistent system. It is introduced on the basis of a wave energy flux conservation. The solution is shown in the Appendix.

Miche's criterion can be valid for a breaking criterion of regular waves on the coexistent system, as being pointed out by Iwagaki⁹⁾ and Sakai¹⁰⁾.

$$\left(\frac{H}{L}\right)_b = \alpha \tanh(kh)_b \quad (14)$$

where subscript b indicates the quantities of the breaking point. The value of α is equal to 0.142 in the case of only wave action. But in the wave-current coexistent system, its value is inclined to decrease according to the increase of the velocity. The breaking point can be calculated by using the ratio of water depth to wave length obtained from the wave height calculation mentioned above.

3.2 Wave height distribution in post-breaking region

In order to obtain the wave height distribution in the post-breaking region, it was assumed that breaking wave has the same process as that of the energy dissipation in bores. The energy loss per unit width of bore is given by

$$\Delta E' = \frac{1}{4} \rho g (h_2 - h_1)^3 \sqrt{\frac{g(h_1 + h_2)}{2h_1h_2}} \quad (15)$$

where h_1 and h_2 are the water depths before and after bore, respectively. The energy loss¹¹⁾ per unit length can be represented by the following equation(16) on the basis of the long wave assumption.

$$h^2 = h_1 \cdot h_2$$

$$\Delta E = \frac{\Delta E'}{L} = \frac{\Delta E'}{CT} = \frac{B}{4} \frac{\rho g H^2}{T} \left(\frac{H}{h} \right) \tag{16}$$

where B is

$$B = \frac{(h_2 - h_1)^3}{H^3} \tag{17}$$

where H is the wave height at a given point in the surf zone.

The wave energy flux taking the mean energy level as a reference on the wave-current coexistent system was given by Jonsson¹²⁾. That is,

$$E = \frac{1}{8} \rho g H^2 (C_g - U_f) \left(1 - \frac{U_f}{C} \right) \tag{18}$$

where C and C_g are the relative wave celerity and the relative wave group celerity to the steady flow, respectively. They can be obtained by use of equation(5). In a shallow water, this equation becomes,

$$E = \frac{1}{8} \rho g H^2 \left(\sqrt{gh} - U_f \right) \left(1 - \frac{U_f}{\sqrt{gh}} \right) \tag{19}$$

Based on the assumptions discussed above, the wave height after breaking is able to be given by the energy flux conservation equation.

$$\frac{dE}{dx} + \Delta E = 0 \tag{20}$$

The x-axis is taken as pointing onshore direction. In order to calculate the wave height distribution in the surf zone for an arbitrary bottom configuration, we performed a numerical solution using equations(16) and (19). In the breaking waves, a turbulent kinetic energy is produced in the surface roller. In addition, turbulence is also induced by the systematic eddy near the breaking point. Consequently, the value of B in equation(16) depends on the location of the surf zone. However, the value on the wave-current coexistent system could not be known in detail. Therefore, the following equations, which were given for a non-coexistent system by Mase¹³⁾, had to be used.

i) In cases that $m > 1/20$

$$0.9 < h/h_b \leq 1.0 : B = 1$$

$$0.6 < h/h_b \leq 0.9 : B = 13 - \frac{40}{3} \frac{h}{h_b} \tag{21}$$

ii) In cases that $m < 1/20$

$$\begin{aligned} 0.6 < h/h_b < 1.0 & : B = 11 - 10 \frac{h}{h_b} \\ h/h_b \leq 0.6 & : B = 5 \end{aligned} \quad (22)$$

where h_b is the breaking water depth and m is the beach slope.

IV. Prediction of bottom profile transformation

The continuity equation for the bottom material is indicated as follows.

$$\frac{\partial z_b}{\partial t} = - \frac{\partial h}{\partial t} = - \frac{\partial q_{net}}{\partial x} \quad (23)$$

where z_b is the bottom level taking the still water level as a reference, and t is the elapsed time from the beginning of the wave-current action. In the practical numerical analysis, the following equation⁴⁾ was employed to restrain the appearances of radical irregular bottom profiles and steep gradients of the bottom more than the angle of repose of the immersed sand. These phenomena may not occur in real beaches.

$$\frac{\partial z_b}{\partial t} = - \frac{\partial}{\partial x} \left(q_{net} - \epsilon_s |q_{net}| \frac{\partial z_b}{\partial x} \right) \quad (24)$$

where ϵ_s is the positive constant. In addition, we used a finite difference method in which staggered mesh scheme is applied to equation(24). The stability of the calculus is indicated by

$$\Delta t \leq \frac{1}{2} \frac{\Delta x^2}{\epsilon_s |q_{max}|} \quad (25)$$

where q_{max} is the maximum value of q_{net} .

V. Comparison between experimental and calculated results

The comparison between the experimental and the calculated results will be discussed in this chapter. Assuming a river mouth as shown in Fig.2, the experiments on the wave-current coexistent system were carried out under the conditions as listed in Table 1. The experimental apparatus consisted of a piston-type wave maker and a pump for the generation of the steady flow in a wave tank(30m long, 1.0m high, and 0.6m wide).

5.1 Method of experiment

A model was formed out of the sand listed in Table 1. It was composed of two parts; the river mouth(4m long, flat) and the sloping beach(12m long, 1/20). The wave height and the change of bottom profile induced by wave and steady flow were measured with spaces of 1cm by use of wave gauge and sand-level-meter which were loaded on the observation truck.

Table 1 Condition of experiments.

Case	(1) $q_c(\text{cm}^2/\text{s})$	(2) $H_0(\text{cm})$	(3) $T(\text{s})$	(4) $h(\text{cm})$	(5) (cm/s)	(6) Fr	(7) $d_{50}(\text{mm})$	(8) S	C_s
A	197.2	6.49	2.2	4.38	45.02	0.69	0.37	1.72	2.96
B	138.2	6.49	2.2	4.86	28.43	0.41	0.37	1.72	2.96
C	35.8	4.68	2.2	6.96	5.13	0.062	0.28	1.44	2.57
D	133.6	17.51	1.6	8.25	16.20	0.18	0.28	1.44	11.86

- (1): discharge per unit width
- (2): wave height
- (3): wave period
- (4): depth of river mouth
- (5): velocity at river mouth
- (6): Froude number
- (7): median diameter of sand
- (8): specific gravity of immersed sand

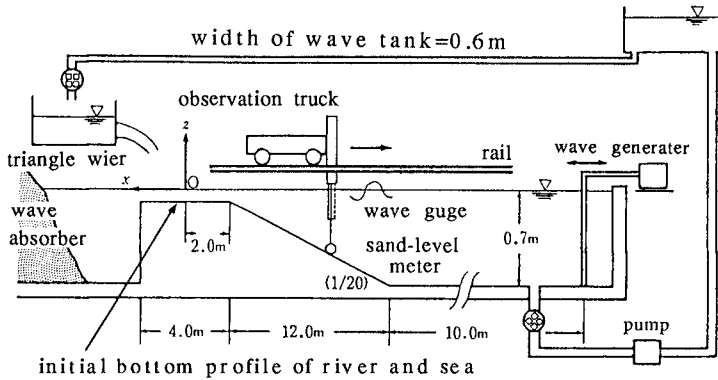


Fig.2 Schematic drawing of experimental apparatus for wave-current coexistent system.

The net transport rate of sand drift was calculated from the profile change at 20-minute intervals by use of the difference equation of equation(23). In Table 1, the waves which caused an accretion of the beach were worked for Cases of A, B and C, and in the Case of D the wave produced an erosion of the beach. In addition, the classification of the wave-type for two-dimensional laboratory beach transformation in terms of a parameter, C_s , was used here. It was proposed by Sunamura and Horikawa¹⁴⁾.

$$\frac{H_0}{L_0} = C_s \cdot m^{-0.27} \cdot \left(\frac{d}{L_0}\right)^{0.67} \tag{26}$$

where H_0 is the deep water wave height and L_0 is the deep water wave length. If $C_s < 4$, the beach is accreted, while if $C_s > 8$, the beach is eroded.

5.2 Wave height distribution

Figs.3(a) through (d) show the comparison between the experimental and calculated results of the wave height distribution. In determining the breaking height on the wave-current coexistent system for the numerical calculation, the value of α in equation(14) was taken as 0.132. The bottom profiles at the time of wave height measurement are also shown in the figures. These bottom profiles are used for the calculation of the wave height. Figs.3(a) through (c) and (d) correspond to cases of plunging breaker and spilling breaker, respectively. The calculated results for the wave height near the breaking point in the case of spilling breaker have a tendency to give smaller values than the experimental results as shown in Fig.3(d). But good agreements are found between the experimental and calculated results in the cases of plunging breaker. From the above results, it may be concluded that the wave height calculation model succeeds fairly well in predicting the experimental results.

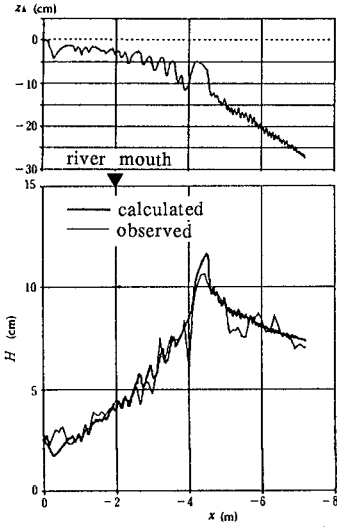
5.3 Distribution of sand transport rate

Figs.4(a) through (d) show the comparison between the experimental and calculated distributions of the sand transport rate. Here, in order to match with the wave height calculation, the bed velocity amplitude U_w in the pre-breaking region was calculated by use of the third order approximate solution of Stokian wave. In the post-breaking region, U_w is obtained using the linear long wave theory.

The procedures of the calculation for the transport rate, q_{net} , will be illustrated in the following;

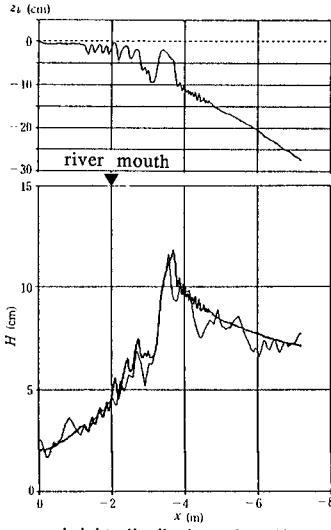
- 1) The local transport rate at a given point is calculated by use of equations(1) through (7) under the assumption of $A_f = |A_w| = 1$.
- 2) The predominant direction of transport rate, q_w , at a given point is judged with equations(9) through (13). If the direction is offshore, A_w is equal to 1, while if the direction is onshore, A_w is equal to -1.
- 3) Comparing the peak value of the calculated distribution of transport rate with that of observed distribution and finding the both peak values to be equal each other, then the $A_f (= |A_w|)$ is required one.
- 4) The final value of the transport rate at the each point is obtained multiplying the value of the transport rate given in procedure 1) by $A_f (= |A_w|)$ gotten above.

(a) Case A
bottom profile formed by action of wave
and steady flow for 60 minutes.



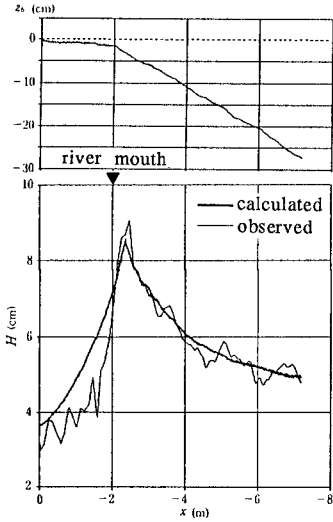
wave height distribution after 60 minutes.

(b) Case B
bottom profile formed by action of wave
and steady flow for 40 minutes.



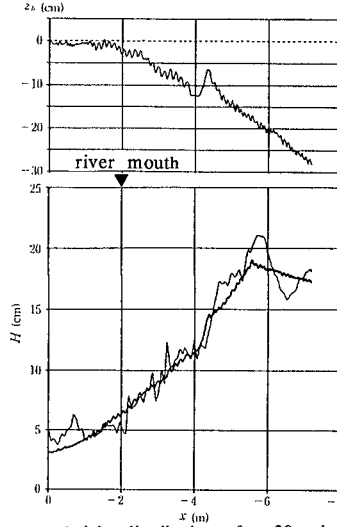
wave height distribution after 40 minutes.

(c) Case C
bottom profile just before action of wave
and steady.



wave height distribution after 1 minutes.

(d) Case D
bottom profile formed by action of wave
and steady flow for 20 minutes.



wave height distribution after 20 minutes.

Fig.3 Comparison between calculated and experimental results of wave height.

In determining the direction of sand drift at the each point, the value of γ in equation(11) is taken as 0.32 for the numerical calculation. In the calculations, the both values of A_f and $|A_w|$ are taken to be equal for all over the surf zone. The values obtained from the experiments are shown in Fig.5.

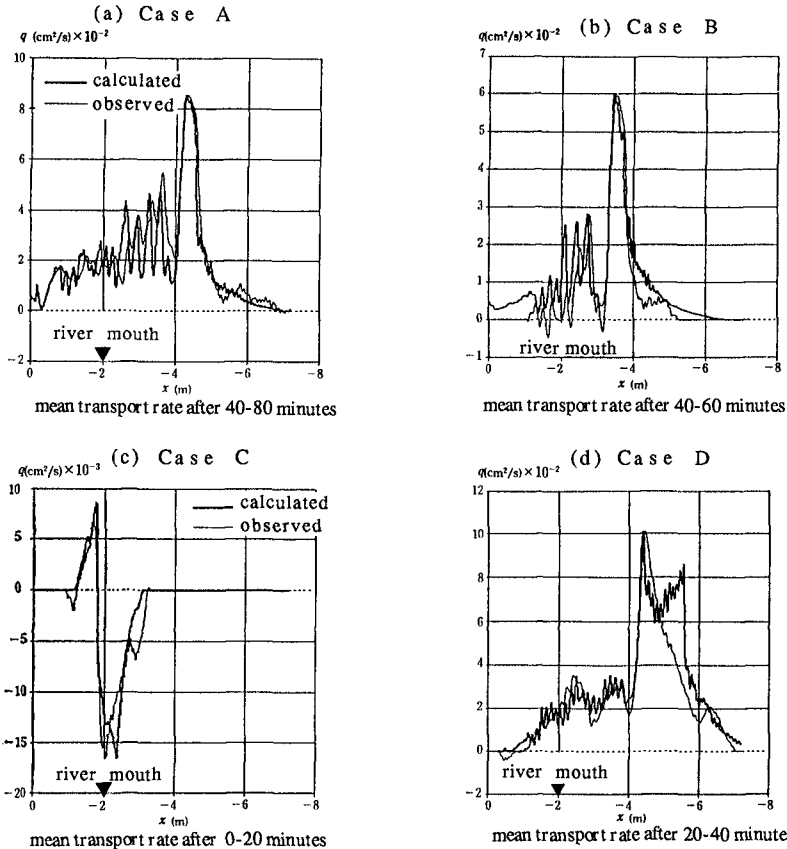


Fig.4 Comparison between calculated results and experimental results of distributions of on-offshore transport rate.

5.4 Beach profile transformation

Fig.6 shows an example of the calculated bottom profile, and it is compared with the experimental data in Case of C. The profile was formed under the action of wave and current for 20 minutes, and the initial profile which was observed just before beginning of wave-current action is shown in Fig.3(c). Using the calculated distributions of the wave height and the sand transport rate, the prediction of bottom transformation was done at intervals of 1cm

from the difference equation of equation(24) under the conditions of $\epsilon_s=2.0$ and $\Delta t=10\text{sec}$. The value of A_f or A_w for the sand transport rate calculation was obtained from the experimental results as shown in Fig.5. In average, the profile calculated by use of this model agrees well with that obtained from the experiment.

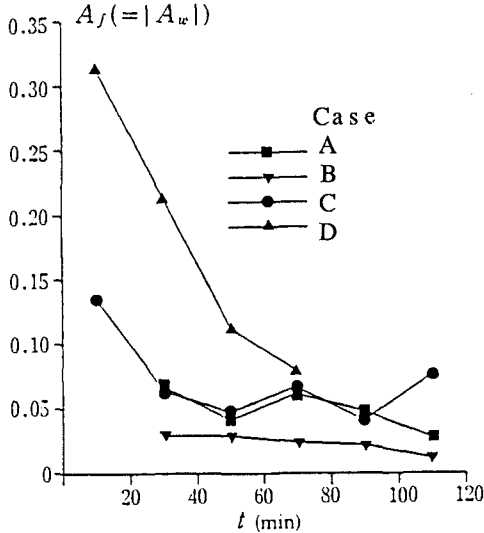
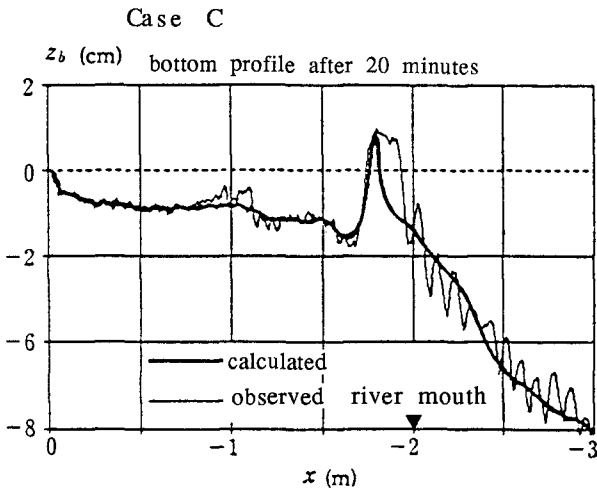


Fig.5 Change of value $A_f (= |A_w|)$ with elapsed time.



initial profile of bottom is shown in Fig.3(c)

Fig.6 An example of calculation for beach transformation due to wave and current.

VI. Conclusion

The conclusions in this study are indicated as follows;

- 1) The local transport rate of sand drift in the both regions of pre-breaking and post-breaking could be estimated with the application of the bed load formula proposed by Watanabe.
- 2) The predominant direction of sand drift could be recognized using the judgment equation which was derived from our previous study.
- 3) The distribution of wave height on the post-breaking region could be analyzed by use of a bore model. And the distribution in the pre-breaking region could be obtained from the third order approximate solution of Stokian wave on the coexistent system.
- 4) The prediction of the bottom transformation in the two-dimensional coexistent system could be done by use of the equation of continuity of the sand transport rate.
- 5) The results obtained by this analytical model agreed well the experimental results of laboratory. That is, the model developed in this paper is capable of describing aspects of two-dimensional sand movement, wave deformation and beach transformation on a wave-current coexistent system.

Appendix

(1) The friction law for the wave-current coexistent system

The next equations indicate the friction law given by Tanaka and Shuto⁵⁾ on the assumption of rough bottom.

(i) Friction coefficient

$$f_{cw} = 2B \left(\frac{\bar{u}_c}{\hat{u}_w} \right)^2 + 4BC \frac{\bar{u}_c}{\hat{u}_w} \cos \alpha + 2C^2$$

$$B = \frac{\kappa}{\ln(h/z_0) - 1}$$

$$C = \begin{cases} \frac{\kappa}{\pi} \left\{ 0.25 + 0.101 \left(\ln \frac{\sigma z_0}{\hat{u}_w} - \frac{1}{2} \ln f_{cw} + 0.24 \right)^2 \right\}^{-1/2}, & \frac{\hat{u}_w}{\sigma z_0} \geq 50 \\ 0.738 f_{cw}^{-1/4} \left(\frac{\hat{u}_w}{\sigma z_0} \right)^{-0.408}, & 50 \geq \frac{\hat{u}_w}{\sigma z_0} \geq 10 \end{cases}$$

where f_{cw} is the friction coefficient, z_0 is the roughness length, \bar{u}_c is the velocity averaged over the section of steady flow, \hat{u}_w is the bottom velocity amplitude of orbital motion induced by wave and σ is the angular frequency.

(ii) Maximum Shear stress on the coexistent system

$$\tau = \frac{1}{2} \rho f_{cw} \hat{u}_w^2$$

where τ is the maximum shear stress acting to the bottom.

2) *The third order approximate solution of Stokian wave on the wave-current coexistent system.*

The next equations indicate the third order approximate solution of Stokian wave given by Sakai, Saeki and Ozaki⁸⁾.

(i) Velocity potential

$$\Phi = Ux + \frac{C-U}{k} \{ (\lambda A_{11} + \lambda^3 A_{13}) \times \cosh k(h+z) \sin\theta + \lambda^2 A_2 \cosh 2k(h+z) \sin 2\theta + \lambda^3 A_3 \cosh 3k(h+z) \sin 3\theta \}$$

$$\zeta = \frac{1}{k} (\lambda f_1 \cos\theta + \lambda^2 f_2 \cos 2\theta + \lambda^3 f_3 \cos 3\theta)$$

$$B = B_0 + \lambda B_1 + \lambda^2 B_2 + \lambda^3 B_3$$

$$C = C_0 + \lambda C_1 + \lambda^2 C_2 + \lambda^3 C_3$$

$$k = 2\pi/L, \lambda = ka, \theta = k(x - Ct)$$

$$\begin{aligned} A_{11} &= \frac{1}{\sinh\beta} & , & & f_2 &= \frac{1}{4} \frac{\cosh\beta}{\sinh^3\beta} (\cosh 2\beta + 2) \\ A_{13} &= -\frac{\cosh^2\beta}{8\sinh^5\beta} (5\cosh^2\beta + 1) & , & & f_3 &= \frac{3}{64} \frac{8\cosh^6\beta + 1}{\sinh^6\beta} \\ A_2 &= \frac{3}{8} \frac{1}{\sinh^4\beta} & , & & B &= \frac{U^2}{2} + \frac{a^2 g}{2} k \frac{1}{\sinh 2\beta} \\ A_3 &= \frac{1}{64} \frac{11 - 2\cosh 2\beta}{\sinh^7\beta} & , & & (C-U)^2 &= \frac{g}{k} \tanh\beta \left(1 + \frac{\lambda^2 \cosh 4\beta + 8}{8 \sinh^4\beta} \right) \\ f_1 &= 1 & , & & \pi \frac{H}{L} &= \left(\lambda + \frac{3}{64} \lambda^3 \frac{8\cosh^6\beta + 1}{\sinh^6\beta} \right) \end{aligned}$$

$$\beta = kh$$

where Φ is the velocity potential, ζ is the surface level variation, L is the wave length and H is the wave height.

(ii) Energy flux

$$W = \rho \frac{C}{k} \{ U(C-U) Q_1 + (C-U)^2 Q_2 \}$$

$$Q_1 = \lambda^2 \frac{1}{\sinh^2\beta} \left[\frac{1}{2} \sinh\beta \cosh\beta + \frac{\lambda^2}{3} \frac{\cosh\beta}{\sinh^5\beta} \{ -4\cosh^6\beta + 20\cosh^4\beta - 16\cosh^2\beta + 9 \} \right]$$

$$\begin{aligned} Q_2 &= \lambda^2 \frac{1}{\sinh^2\beta} \left[\frac{1}{4} (\sinh\beta \cosh\beta + \beta) + \frac{\lambda^2}{8} \left\{ \frac{1}{8\sinh^6\beta} (\sinh\beta \cosh\beta + \beta) \right. \right. \\ &\quad \times (-20\cosh^6\beta + 16\cosh^4\beta + 4\cosh^2\beta + 9) + \frac{\cosh\beta}{4\sinh^3\beta} \\ &\quad \left. \left. \times (16\cosh^4\beta + 2\cosh^2\beta + 9) \right\} \right] \end{aligned}$$

where W is the energy flux, U is the velocity of steady flow and C is the relative wave celerity.

References

- (1) Inman, D. L. and A. J. Bowen: Flume experiments on sand transport by waves and Currents, Proc. 8th Conf. on Coastal Engng., pp.137-150, 1963.
- (2) Abou-Seida, M. M: Sediment transport by waves and current, Tech. Rep. No.HEL-2-7, Univ. of California, Berkley, 1964.
- (3) Tanaka, H., H. Ozasa and A. Ogasawara: Experiments on sand movement by waves and current, Rep. Port & Harbor Res. Inst., Vol.12, No.4, 1973 (in Japanese).
- (4) Watanabe, A., K. Maruyama, T. Shimuzu and T. Sakakiyama: Numerical prediction model of three-dimensional beach deformation around coastal structures, Proc. of Japanese Conf. on Coastal Engng., pp.406-410, 1984(in Japanese).
- (5) Tanaka, H. and N. Shuto: Friction coefficient for a wave-current coexistent system, Coastal Engng. in Japan. Vol.24, pp.105-128, 1981.
- (6) Sunamura, T: Prediction of on-offshore sediment transport rate in the surf zone including swash zone, Proc. of Japanese Conf. of Coastal Engng., pp.316-320, 1984(in Japanese).
- (7) Kinose, K. and S. Okushima: Sand transport near sand bar on two-dimensional wave current coexistent system, Proc of '87 Annual Meeting of Japan Society of Irrigation, drainage and Reclamation Engng., pp.68-69, 1987(in Japanese).
- (8) Sakai, S. and A. Ozaki: Effect of Current on wave Shoaling, Proc. of 29th Japanese Conf. on Coastal Engng., pp.70-74, 1982(in Japanese)
- (9) Iwagaki, Y, T. Asano, T. Yamanaka and F. Nagai: Fundamental study on breaking of waves due to currents, Proc. of 27th Japanese Conf. on Coastal Engng., pp.30-34, 1980(in Japanese).
- (10) Sakai, S., K. Ota, H. Oba, T. Kuribayashi and H. Saeki: Shoaling of irregular waves affected by opposing current, Proc. of Japanese Conf. on Coastal Engng., pp.224-228, 1985(in Japanese).
- (11) Mase, H., A. Matsumoto and Y. Iwagaki: Calculation of random wave transformation in shallow water, Proc. of JSCE, No.375 /II-6, pp.221-230, 1986(in Japanese).
- (12) Jonsson, I.G and J.D. Wang: Interaction between wave and current, Proc. of 12th Conf. on Coastal Engng., pp.489-507, 1970.
- (13) Mase H. and Y. Iwagaki: Wave height distributions and wave grouping in surf zone, Proc. of 18th Conf. on Coastal Engng., pp.58-69, 1982.
- (14) Sunamura, T. and K. Horikawa: Two-dimensional beach transformation due to waves, Proc. of 14th Conf. on Coastal Engng., pp.920-938, 1974.